

## Design of organic solar cells based on a squaraine dye as electron donor

S. Kitova\*, D. Stoyanova, J. Dikova, M. Kandinska<sup>1</sup>, A. Vasilev<sup>1</sup> and V. Mankov

*Institute of Optical Materials and Technologies "Acad. J. Malinowski",  
Bulgarian Academy of Sciences, Acad. G. Bonchev Str., Bl.109, 1113 Sofia, Bulgaria*

*<sup>1</sup>Sofia University "St. Kliment Ohridski, Faculty of Chemistry and Pharmacy,  
James Bourchier Blvd., 1164 Sofia, Bulgaria*

Received October 10, 2016; Revised November 21, 2016

Optical modelling based on transfer matrix method has been carried out to design small molecule BHJ organic solar cells with better performance. The active layers represent blends of in-house synthesized squaraine dye Sq1 as electron donor and soluble fullerene derivative PC<sub>61</sub>BM ((6,6)-phenyl C<sub>61</sub> butyric acid methyl ester) as acceptor. The solar photon absorption in Sq1/PC<sub>61</sub>BM layers with different weight ratio has been simulated and the possible maximum short circuit photocurrent ( $J_{sc}^{max}$ ) in devices with standard and inverted architecture has been calculated. It is found that the inverted device stacks show larger calculated  $J_{sc}^{max}$  compared to the standard device structure. Modelling of the optical field distribution in the different device stacks proved that this enhancement originates from an increased absorption of incident light in the active layer, and hence from the increased exciton generation rate. Simultaneously, it is established that the effect of the ZrO<sub>2</sub> optical spacer to the increase of  $J_{sc}^{max}$  is less expressed in inverted device stacks than in standard ones. Finally, the results obtained are discussed with a view to finding the optimal design of real BHJ cells based on Sq1/PC<sub>61</sub>MB active layers.

**Keywords:** bulk heterojunction organic solar cells, inverted solar cell, squaraine dye, optical modelling

### INTRODUCTION

Recently, the organic solar cells (OSCs) based on polymer or low molecular weight semiconductors are subject of continuously growing interest as promising low-cost alternative of Si-solar cells that still dominate the market [1]. Contemporary OSCs devices are based on a heterojunction that results from the contact between electron donor (D) and electron acceptor (A) materials. D/A heterojunctions can be created with two main types of architecture: bilayer heterojunction and bulk heterojunction (BHJ) that is now regarded as the most promising approach to obtain high performance devices [1].

The most key element of the multilayered OSCs structure are the active layers, composed by two components – donor and acceptor. In BHJ cells the active layer represents a blend of donor and acceptor that provides larger D/A interface where generation of charge carriers takes place [2]. Till now, the best efficiency OSCs contain fullerene C<sub>60</sub> and especially its soluble derivative PCBM ((6,6)-phenyl C<sub>61</sub> butyric acid methyl ester) as acceptor, which seem without alternative in the near future

[3]. As per the type of the electronic donors the organic cells are conditionally divided into polymer and low-molecular (M below 100) ones. Juxtaposing the properties of these two classes of organic semiconductors reveals that the low-molecular ones possess higher purity, better reproduction of the main physicochemical and optical properties, higher carrier mobility, better defined molecular structure and exactly determined molecular weight [1, 4]. All the pointed advantages have generated unprecedented interest and intensive research in the recent years, aiming at development and exploring of new electron donors for producing the so-called "small molecule" OSCs. However, even though the highest power conversion efficiency (PCE) of 9.96 % was obtained very recently it is still considerable lower than that of inorganic solar devices [5]. Obviously, further research efforts are needed to obtain cells with better performance and prolonged lifetime. This requires the optimization of several factors which determine the cell efficiency, such as molecular structure of the donor materials and their optical and electrical properties, active layer nanomorphology, ratio between the donor and acceptor moieties in the BHJ film, concentration of

\* To whom all correspondence should be sent:  
E-mail: skitova@iomt.bas.bg

the blend D/A solution and last but not least the device architecture [6].

In our previous work [7] the potentiality of a synthesized by us symmetrical n-hexyl substituted squaraine dye (labeled as Sq1) for using as electron donor component in BHJ organic solar cells with conventional structure (here referred to as “standard”) has been studied from the optical point of view. The soluble n-type fullerene PC<sub>61</sub>MB was chosen as acceptor. The results of optical modelling performed indicate that the optimal thickness of the blended Sq1/PC<sub>61</sub>MB active layer is about 100 nm, which provides an efficient overlapping of the total absorption with solar spectrum in the range between 580 and 900 nm [7]. It is known, however that due to the short exciton diffusion length and low charge carrier mobility of organic materials, the thickness of the active layers should be considerably smaller [8]. To compensate the lower absorption in the thinner active layers a smart design strategy has been applied [9], consisting of the insertion of optical spacers [10] and the use of different contact materials which reduce the parasitic absorptions [11]. Moreover, to improve the charge collection, functional layers are inserted to modify the interfaces between the active layers and the respective electrodes [1]. Following the above strategy we have found that the insertion of ZnO or C60 spacer layer with optimal thicknesses significantly enhances  $J_{sc}^{max}$  for active layers thinner than 50 nm, which is mainly due to the improved light absorption by a factor of 5 to 10. Simultaneously, the optical effect of inserted PEDOT:PSS hole transporting layer was found to be negligible for thicknesses of Sq1/PCMB layers below 100 nm [7].

Recently, there have been extensive investigations on the so-called “inverted architecture” of polymer solar cells (PSCs), where the polarity of charge collection is the opposite of the conventional design [12, 13]. The implementation of the inverted cell structure requires the introduction of a buffer layer from metal oxide, mostly ZrO<sub>2</sub>, ZnO, TiO<sub>2</sub> etc., for improving the function of the transparent ITO electrode as cathode, and a substitution of Al electrode with higher work function metal like Au, Ag, Pt, etc., which serves as anode [13]. Compared with conventional PSCs, the inverted type devices demonstrate better long-term ambient stability by avoiding the need for the corrosive and hygroscopic PEDOT:PSS and low-work-function metal cathode, both of which are detrimental to device lifetime [14]. It has also been shown that the inverted design

provides superior solar cell performance, which was attributed to different absorption profiles with reduced parasitic absorption in polymer:fullerene solar cells [15]. However, the efficiency of this architecture in small molecule organic cells has hardly been investigated.

In the present work, the potential photovoltaic performance of BHJ solar cells with Sq1/PC<sub>61</sub>BM active layer and different design was projected by optical modelling based on transfer matrix method. For the purpose the simulated solar photon absorption in blended with different weight ratio Sq1/PC<sub>61</sub>BM active layers and the calculated maximum short circuit current  $J_{sc}^{max}$  for cells with standard and inverted architecture were compared. Besides, the impact of ZrO<sub>2</sub> and MoO<sub>3</sub> optical spacers on the calculated  $J_{sc}^{max}$  values were also estimated.

## EXPERIMENTAL DETAILS

The symmetrical n-hexyl substituted squaraine dye 2-(5-(((2,2-diphenylhydrazono) methyl)-1-hexyl-1H-pyrrol-2-yl)-4-(5-(2,2-diphenylhydrazono)-ylidenemethyl)-1-hexyl-2H-pyrrol-1-ium)-3-oxocyclobut-1-enolate, labeled as Sq1) was in-house synthesized [7] by optimizing a method proposed recently in the literature [16, 17].

Single Sq1 dye and blended Sq1/PC<sub>61</sub>MB films with different weight ratios (1:1, 1:2, 1:3) were prepared from solution of the compounds in chloroform by spin coating in glove box. The experimental details are described in [7]. Optical constants of the blended Sq1/PC<sub>61</sub>MB films were determined with a high accuracy on the basis of three spectrophotometric measurements at normal incidence of light - transmittance T and reflectance R<sub>f</sub> and R<sub>m</sub> of the films, deposited on transparent (BK7) and opaque (Si wafers) substrates, respectively [18].

Optical modeling of a BHJ device stack was carried out using the transfer matrix formalism, based on the Fresnel formulas for the several interfaces occurring in the cell. This approach has been explained in full detail in the literature [19, 20]. In our work a Matlab script developed by Burkhard and Hoke, which treats the case of normal incidence of light, was applied [21]. The absorption distribution for each wavelength over the film thickness has been calculated in the wavelength range 350 – 900 nm.

Knowing the power of incoming AM 1.5 solar spectrum, the exciton generation rate per unit volume G(x) at each position x is described by

$$G(x) = \int_{\lambda_1}^{\lambda_2} \frac{\lambda}{hc} Q_{act}(x,\lambda) d\lambda$$

where the  $Q(x, \lambda)$  is the time average of the energy dissipation per unit time at the position  $x$  and wavelength  $\lambda$ ,  $h$  is Plank's constant and  $c$  is the speed of light [19]. Further integration over the film thickness results in the total number of absorbed photons. The possible maximum short circuit current density  $J_{sc}^{max}$  was calculated assuming that each absorbed photon results in a collected electron i.e. the internal quantum efficiency, IQE, equals one [21].

The two types of architectures of the modelled solar cells are shown in Fig. 1. In the standard device configuration (Fig. 1a), the active layer is sandwiched between PEDOT:PSS and  $ZrO_2$  covered with Al. For the inverted devices (Fig. 1b), the active layer is embedded between the electrons selective  $ZrO_2$  and the holes selective  $MoO_3$  layers,

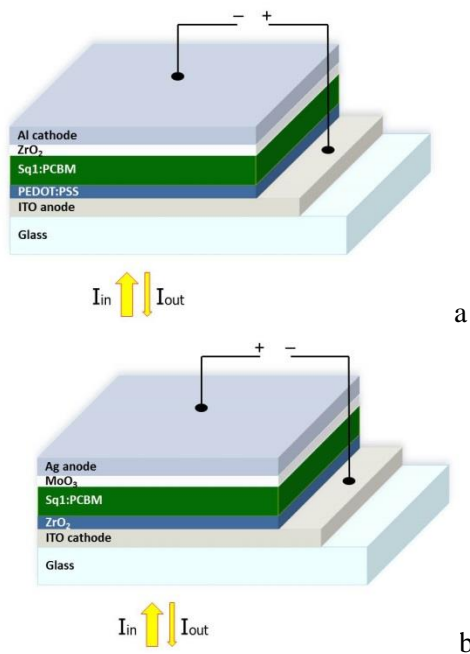


**Fig. 1.** Scheme of BHJ organic solar cells with: a) standard structure; b) inverted structure.

covered with Ag metal contacts. The optical modelling was performed for both BHJ cell structures, where the light enters through the glass substrate, sequentially passing the buffers and active layers. Then the light is reflected back from the metal electrode and finally leaves the solar cell partly at the front again. In all calculations the thicknesses of ITO and Ag electrodes were set to 100 nm and those of PEDOT:PSS to 60 nm. We have used literature data for the optical constants of ITO, Al and  $ZrO_2$  [22]. The optical constants of PEDOT:PSS, Ag and  $MoO_3$  films were determined

experimentally by applying the same procedure as for Sq1 dye. For the purpose 50 nm thick films were spin coated or thermally evaporated in vacuum ( $10^{-4}$  Pa) on glass substrates and Si wafers.

## RESULTS

As a first step in our study the optimal Sq1/PC<sub>61</sub>BM weight ratio in the blended active layers was experimentally determined. This is because of the fact that, as noted above, the ratio between the donor and acceptor moieties in the BHJ film affects strongly the device performance. Fig. 2 presents the absorption spectra of 100 nm films with different Sq1/PC<sub>61</sub>BM weight proportions (1:1, 1:2 and 1:3). As seen, the spectrum of the all samples studied shows absorption of light across a broad range of wavelengths - from ultraviolet to near infrared, with a maximum at 775 nm. The absorption in the range 350 – 600 nm is due to the presence of PC<sub>61</sub>MB in the blended films whilst the main absorption peak is due to electron excitations in the squaraine dye molecules. Reasonably, the height of the main peak decreases with decreasing the content of Sq1 in the blended films studied, being the lowest for 1:3 proportions of the donor/acceptor constituents. Further, the photovoltaic potential of Sq1/PC<sub>61</sub>BM active layers was followed in simple standard cells, ITO/PEDOT:PSS(~60nm)/Sq1:PC<sub>61</sub>BM(~100nm)/Al(~100nm). The current density–voltage (J-V) curves obtained for cells with different Sq1/PC<sub>61</sub>BM ratio in the active layers are shown in Fig. 3. It is seen that the weakest photovoltaic response is observed for the active layer with 1:1 ratio of the donor and acceptor moieties. Obviously, this film has very low potential for using as active layer it the cells studied, despite its higher absorption. The two other Sq1/PC<sub>61</sub>BM films (1:2 and 1:3) have almost the same relatively stronger response which was the reason to continue our investigation with them.

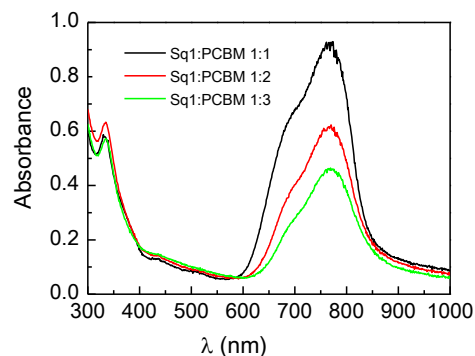


**Fig. 2.** Absorption spectra of 100 nm thick Sq1/PC<sub>61</sub>MB films with different D/A weight ratio.

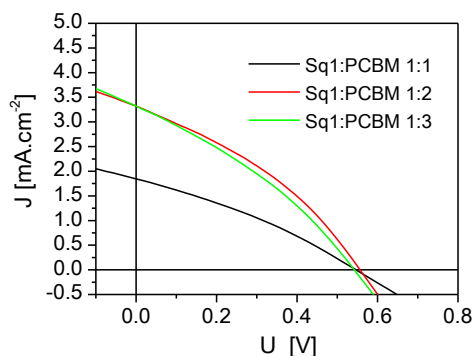


**Fig. 3.** J-V curves for conventional BHJ cells at different weight ratio of the Sq1/PC<sub>61</sub>MB active layers.

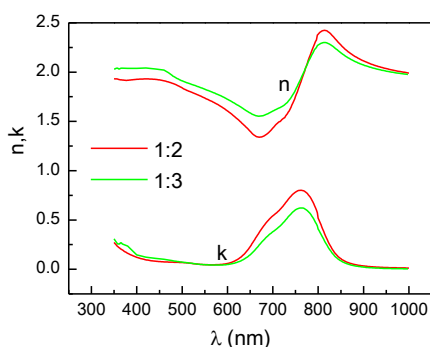


**Fig. 4.** Refractive index (n) and extinction coefficient (k) spectra of blended Sq1/PC<sub>61</sub>MB films.

Fig. 4 shows the spectral dispersions of refractive index (n) and extinction coefficient (k) for blended Sq1/PC<sub>61</sub>MB layers with 1:2 and 1:3 weight ratio. On their basis, the optical absorption profiles for standard and inverted devices, each with 100 nm thick Sq1/PC<sub>61</sub>MB active layer, were calculated and can be compared in Fig. 5. Fig. 5a presents spectral dependence of total absorption within the active layer, while the exciton generation rate  $G_x$  under AM 1.5G illumination versus position in the active layer is shown in Fig. 5b. In the calculations the photon to exciton conversion efficiency is assumed to be one meaning that every single photon absorbed in the active layer initially creates an exciton. It is seen that the inverted structure can harvest more photons from solar spectra than the standard devices. Besides, the generation profile is shifted towards the back metal electrode and the formation of excited states near the back electrode is considerably larger for inverted cell geometry. Hence, the systematical optical modeling studies showed that the inversion of the multilayered cell structure causes both the slight shift of the maximum of the electric field towards the back electrode and the increase of the overall modulus throughout the whole active layer.

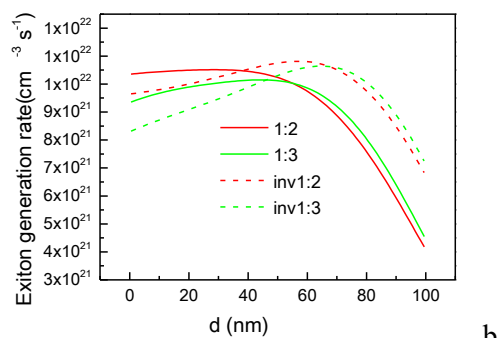
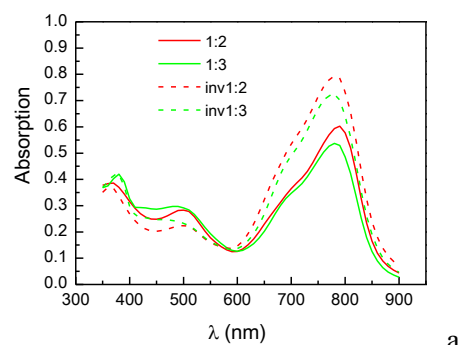


**Fig. 5.** Comparison of calculated optical absorption profiles for devices with standard and inverted structure. The thicknesses of buffer layers ZrO<sub>2</sub> and MoO<sub>3</sub> were set to 20 nm. a) Fraction of incident light absorbed in 100 nm thick Sq1/PC<sub>61</sub>MB active layer in dependence of wavelength; b) Exciton generation rate in 100 nm thick active layer under AM 1.5G illumination as a function of position within the active layer;

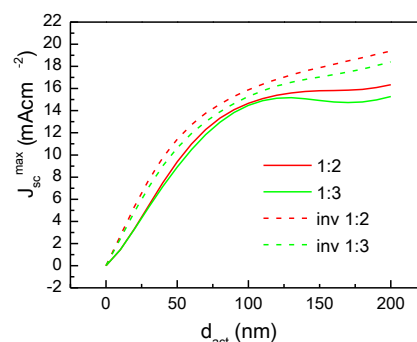


**Fig. 6.** Calculated  $J_{sc}^{max}$  as a function of active layer thickness for the same device structures (as in Fig. 5) under 100 mW cm<sup>-2</sup> AM 1.5G spectral illumination.

Assuming an IQE=1, the maximum short circuit current density  $J_{sc}^{max}$  under AM 1.5G illumination in dependence of Sq1/PC<sub>61</sub>MB layer thickness is depicted in Fig. 6 for both device structures. As seen, the inverted device stack always has a higher  $J_{sc}^{max}$  than the standard one, regardless of the active layer thickness, demonstrating the advantage of the inverted device structure. It should be noted here that these calculations consider the optical properties of the solar cells and not the electrical



necessities of low sheet resistance or prevention of pin hole formation. Nevertheless, they represent a

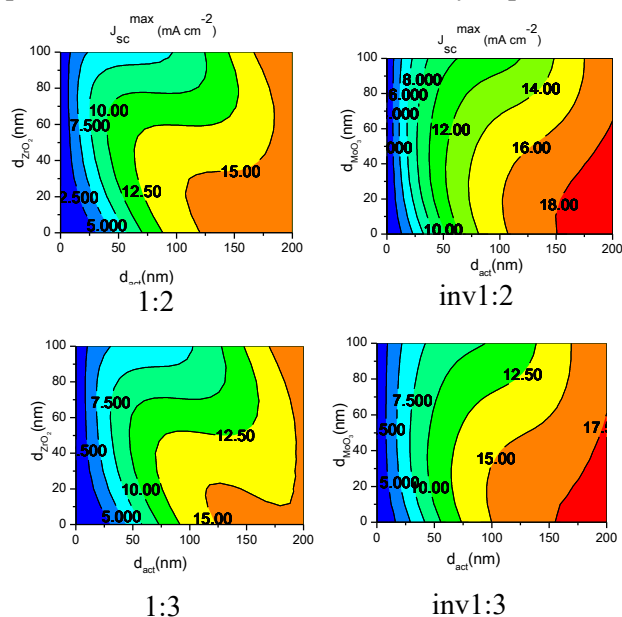


**Fig. 7.** Calculated short-circuit current density  $J_{sc}^{\max}$  contours under  $100 \text{ mW cm}^{-2}$  AM 1.5G spectral illumination as a function of active layers and optical spacer thicknesses for: a) standard device with  $\text{ZrO}_2$  optical spacer and b) inverted device with  $\text{MoO}_3$  optical spacer.

considerable potential improvement of the photocurrent in devices with inverted structure. The dependence of calculated  $J_{sc}^{\max}$  on the thicknesses of the active layers and optical spacer is illustrated in Fig. 7 for standard device with  $\text{ZrO}_2$  spacer/Al electrode and inverted device with  $\text{MoO}_3$  spacer/Ag electrode. According to the simulation results presented, the values of  $J_{sc}^{\max}$  are less dependent on the spacer thickness in the device with inverted structure. On the whole, the effect of optical spacer to the increase in  $J_{sc}^{\max}$  is higher in devices with standard architecture.

## CONCLUSIONS

Optical modelling based on transfer matrix method has been performed to predict and improve the performance of BHJ solar cells with standard and inverted architecture, based on a symmetrical n-hexyl substituted squaraine dye Sq1 as electron donating component in the active layer. The results obtained demonstrate that the inverted device stacks, comprising bulk heterojunction composed of Sq1 donor and  $\text{PC}_{61}\text{BM}$  acceptor with 1:2 and 1:3 proportions, show larger short circuit currents compared to the standard device structure. Obviously, this enhancement originates from the increased absorption of incident light and the

subsequent raise of exciton generation rate within the active layer. This statement is confirmed by the results from modelling of the optical field distribution in device stacks with both types of architecture. On the other hand, the simulations performed show that the impact of the optical spacer on the increase of  $J_{sc}^{\max}$  is less expressed in the cells with inverted design than in standard ones.

Finally, it is worth to mention that the experimental verification of the results obtained is in progress and will be forthcoming in a separate paper.

## REFERENCES

1. A. Mishra, and P. Bauerle, *Angew. Chem. Int. Ed.*, **51**, 2020 (2012).
2. S. Uchida, J. Xue, B. P. Rand, S. R. Forrest, *Appl. Phys. Lett.*, **84**, 4218 (2004).
3. B. Walker, C. Kim, and T. Nguyen, *Chem. Mater.*, **23**, 470 (2011).
4. X. Xiao, G. Wei, S. Wang, G. Zimmerman, Ch. Renshaw, M. Thompson, and S. Forrest, *Adv. Mater.*, **24**, 1956 (2012).
5. B. Kan, Q. Zhang, M. Li, X. Wan, W. Ni, G. Long, Y. Wang, X. Yang, H. Feng, Y. Chen, *J. Am. Chem. Soc.* **136**, 15529 (2014).
6. T. Razykov, C. Ferekides, D. Morel, E. Stefanakos, H. Ullal, H. Upadhyaya, *Solar Energy*, **85**, 1580 (2011).
7. S. Kitova, D. Stoyanova, J. Dikova, M. Kandinska, A. Vasilev, and S. Angelova, *J. Phys.:Conf. Ser.*, **558**, 012052 (2014).
8. G. Burkhard, E. Hoke, and M. McGehee, *Adv. Mater.*, **22**, 3293 (2010).
9. J. Gilot, I. Barbu, M. Wienk, and R. Janssen, *Appl. Phys.Lett.*, **91**, 113520 (2007).
10. Y. Long, *Solar Energy Mater. & Solar Cells* **94**, 744 (2010).
11. Z. He, Ch. Zhong, Sh. Su, M. Xu, H. Wu, and Y. Cao, *Nat. Photonics* **6**, 591 (2012).
12. A. Zhao, S. Tan, L. Ke, P. Lui, A. Kyaw, X. Sun, G. Lo, and D. Kwong, *Solar Energy Mater. & Solar Cells* **94**, 985 (2010).
13. B. Hsieh, Y. Cheng, P. Li, Ch. Chen, M. Dubosc, R. Liang, and Ch. Hsu, *J. Am. Chem. Soc.*, **132**, 4887 (2010).
14. M. Morana, H.Azimi, G. Dennler, H. Egelhaaf, M. Scharber, K. Forberich, J. Hauch, R. Gaudiana, D. Waller, Z. Zhu, K. Hingerl, S. Bavel, J. Loos, and K. Brabec, *Adv. Funct. Mater.*, **20**, 1180 (2010).
15. A. Becke, *Chem. Phys.*, **98**, 5648 (1993).
16. A. Silvestri, M. Irwin, L. Beverina, A. Facchetti, G. Pagani, and T. Marks, *J. Am. Chem. Soc.*, **130**, 17640 (2008).
17. D. Bagnis, L. Beverina, H. Huang, F. Silvestri, Y. Yao, H. Yan, G. Pagani, T. Marks, and A. Facchetti, *J. Am. Chem. Soc.*, **132**, 4074 (2010).

18. Tz. Babeva, S. Kitova, and I. Konstantinov, *Appl. Opt.*, **40**, 2682 (2001).
19. L. Pettersson, L. Roman, and O. Inganä, *J. Appl. Phys.*, **86**, 487 (1999).
20. P. Peumans, A. Yakimov, and R. Forrest, *J. Appl. Phys.*, **93**, 3693 (2003).
21. A. Burkhard, E. Hoke, and M. McGehee, *Adv. Mater.*, **22**, 3293 (2010).
22. Y. Liu, J. Hsieh, and S. Tung, *Thin Solid Films*, **510**, 32 (2006).

## ДИЗАЙН НА ОРГАНИЧНИ СЛЪНЧЕВИ КЛЕТКИ НА ОСНОВАТА НА СКУАРИЛИЕВО БАГРИЛО КАТО ЕЛЕКТРОНЕН ДОНОР

Сн. Китова, Д. Стоянова, Ю. Дикова, М. Кандинска, А. Василев, В. Манков

*Институт по оптически материали и технологии "Акад. Й. Малиновски",  
Българска Академия на науките, ул. "Акад. Г. Бончев", бл. 109, 1113 София, България  
<sup>1</sup>Софийски Университет "Св. Климент Охридски", Факултет по химия и фармация,  
бул. Джеймс Баучер, 1164 Sofia, Bulgaria*

Постъпила на 10 октомври 2016 г.; коригирана на 21 ноември, 2016 г.

(Резюме)

Проведено е оптично моделиране по метода на обърнатата матрица с цел проектиране на нискомолекулни органични слънчеви клетки с обемен хетеропреход и подобрени характеристики. Активният слой представлява смес от синтезирано от нас скуарилиево багрило Sq1 като донор на електрони и разтворим дериват на фулерена PC<sub>61</sub>BM ((6,6)-phenyl C<sub>61</sub> butyric acid methyl ester) като електронен акцептор. Симулирана е абсорбцията на слънчева светлина в активните слоеве с различно Sq1/PC<sub>61</sub>BM съотношение и са пресметнати възможните максимални стойности на тока на късо съединение ( $J_{sc}^{max}$ ) в клетки със стандартна и обърната архитектура. Получените резултати показват, че по-високи стойности на  $J_{sc}^{max}$  могат да се очакват при клетките с обърната структура. Моделирането на разпределението на оптичното поле в клетките с различен дизайн потвърди, че това увеличение се дължи на повишената абсорбция на падащата светлина в активния слой и следователно на по-високата концентрация на екситоните. Установено е също така, че влиянието на оптичния спейсър от ZrO<sub>2</sub> върху повишаването на стойностите на  $J_{sc}^{max}$  е по-силно изразено в стандартните моделни клетки. Резултатите от проведеното изследване са дискутирани с оглед намирането на оптимален дизайн на реални слънчеви клетки с обемен хетеропреход на основата на Sq1/PC<sub>61</sub>MB активни слоеве.